

CONNIE: Coherent Neutrino-Nucleus Interaction Experiment

G. Fernandez Moroni^{**}, J. Estrada^{*}, G. Cancelo^{*}, E. Paolini[†]

^{*}Fermi National Accelerator Laboratory

[†]Inst. de Investigaciones en Ing. Electrica, CONICET

Abstract

The neutrino-nucleus coherent interaction has never been observed because of the very low energy deposition at the detectors. In this paper we present a new experiment that uses very low noise scientific CCDs for looking at this low energy depositions produced by nuclear reactor antineutrinos scattering off a silicon nucleus. The experiment will be placed at Angra Nuclear Power Plant.

Introduction

Neutrino-nucleus neutral current interaction has never been observed. In this process, a neutrino of any flavor scatters off a nucleus transferring some momentum. For low energy neutrinos ($E_\nu < 50\text{MeV}$) the nucleus cross section becomes relatively high compared to other neutrino interactions in that energy range. The standard model cross section for this process is given by:

$$\frac{d\sigma}{dE_{rec}} = \frac{G_F^2}{8\pi} [Z(4\sin^2\theta_w - 1) + N]^2 M^2 \left(2 - \frac{E_{rec}M}{E_\nu^2}\right) |f(q)|^2$$

where M , N and Z are the mass, neutron number and atomic number of the nucleus, respectively, E_ν is the neutrino energy and E_{rec} is the measurable recoil energy of the nucleus, $f(q)$ is the nucleus form factor at momentum transfer q . This form factor can be used in good approximation as $|f(q)| \sim 1$ (the corrections are a few percent only). This formula is applicable at $E_\nu < 50\text{MeV}$ where the momentum transfer (Q^2) is small such that $Q^2 R^2 < 1$, where R is the nuclear size. At low momentum transfer, the nucleon wave function amplitudes are in phase and add coherently, so the cross section is enhanced by $\sim N^2$.

In spite of its large cross section, coherent elastic neutrino nucleus scattering has been difficult to observe due to the very small resulting nuclear recoil energies: the maximum recoil energy is $\sim 2E_\nu^2/M$, which is in the sub-MeV range. However, new ultra-low threshold detectors such as Ge and Si detectors (CCDs) have appeared in recent years. One common characteristic of very low threshold detectors is their relatively small size compared to typical neutrino detectors and therefore their small detection mass. This pushes the use of higher intensity neutrino source so nuclear reactor seems to be a suitable solution for coherent neutrino-nucleus elastic scattering experiments.

The total cross section for a mono energetic neutrino source at energy E_ν is given by

$$\sigma_{Tot} = \frac{G_F^2}{4\pi} [Z(4\sin^2\theta_w - 1) + N]^2 \sim 4.22 \times 10^{-45} N^2 \left(\frac{E_\nu}{1\text{MeV}}\right)^2 \text{cm}^2$$

and is plotted for ^{74}Ge ($N=42$) and ^{28}Si ($N=14$) for the reactor antineutrino energy.

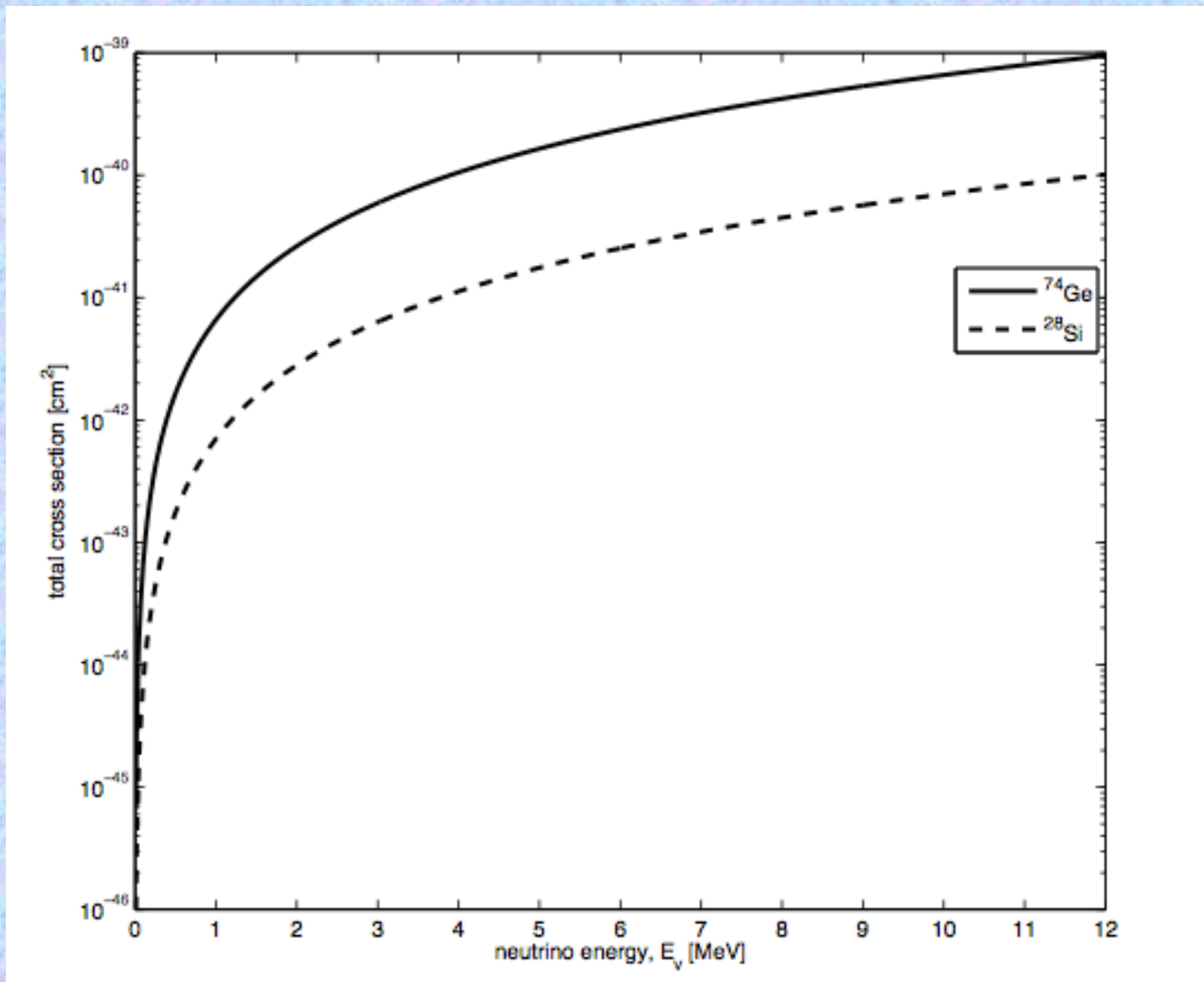


Fig. 1. Total coherent cross section.

Nuclear reactor antineutrino flux

Nuclear reactors emit large numbers of antineutrinos, about 0.3×10^{20} ν_e /seg per GW of thermal power, broadly distributed over energies up to 12 MeV with a peak at 0.5-1 MeV. The neutrinos come out isotropically so the expected flux at a distance L is related to the core yield by the factor $1/(4\pi L^2)$. The modeling of the ν_e spectrum above 3 MeV is consistent with measurements at the $< 5\%$ level, while the low energy portion is subjected to much bigger uncertainties [2]. About $N_{\nu_e} \sim 7.3$ ν_e are produced per reactor fission at steady state operation [3]. Quantity N_{ν_e} receives contribution from many sources, but two of them have the mayor contribution:

$$N_{\nu_e} = F N + U N$$

here $F N \sim 6.1$ ν_e /fission represents summed contribution from beta decays of fission fragments of four fissile isotopes ^{235}U , ^{238}U , ^{239}Pu , ^{241}Pu , and $U N \sim 1.2$ ν_e /fission comes from neutron capture by the ^{238}U .

Antineutrino flux by fissile isotopes

The ν_e 's emitted in power reactors are predominantly produced through β -decays of the fission products, following the fission of the four dominant fissile isotopes: ^{235}U , ^{238}U , ^{239}Pu , ^{241}Pu . Other fissile isotopes such as ^{238}U , ^{240}Pu , ^{242}Pu , etc. contribute less than 0.1% to the fissile isotopes spectrum and can, therefore, be neglected. Each isotope has a different ν_e -yield, ν_e -spectrum and fission rate. Their fission rates also change during the power cycle and hence the ν_e -spectrum changes during burning cycle. The typical ν_e -yield per element fission, as well as their relative contributions per reactor fission are summarized in the following table. The ν_e -yield per element fission was adopted from ref. [4], the relative contributions were taken from ref. [3] depicted for the Kuo-Sheng Nuclear Power station (2.9 GW).

Process	Relative rate per reactor fission	Neutrino yield for each process	Neutrino yield per reactor fission
^{235}U	0.55	6.14	3.4
^{238}U	0.07	7.08	0.5
^{239}Pu	0.32	5.58	1.8
^{241}Pu	0.06	6.42	0.4
$^{238}\text{U}(n,\gamma)$	0.6	2	1.2

The spectrum per fission of each isotope was adopted from ref. [5] and is depicted in the next figure.

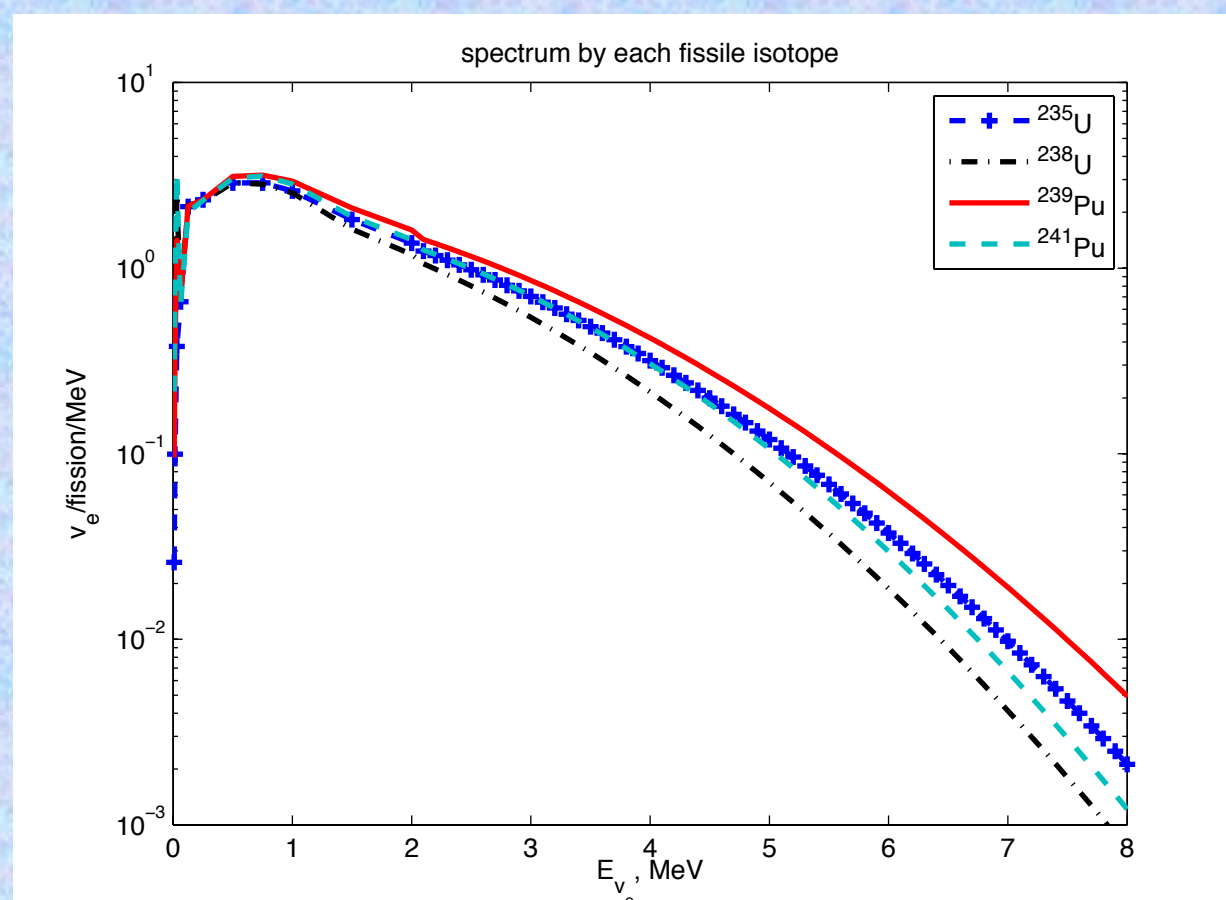


Fig. 2. ν_e -yield per fission for each fissile isotope.

Antineutrino flux by neutron capture in ^{238}U

Nuclear fuel in power reactors contains 95-97% of ^{238}U . ^{238}U absorbs ~ 0.6 neutrons per fission via (n,γ) reaction: $^{238}\text{U} + n \rightarrow ^{239}\text{U} \rightarrow ^{239}\text{Np} \rightarrow ^{239}\text{Pu}$. Two ν_e are produced for the β -decay of ^{239}U . This process contribute $\sim 16\%$ to the total flux. The ν_e -yield and rate per fission at the reactor are also summarized in the table above. The neutrinos produced by this process have energy below 1.3 MeV. The spectrum is plotted in figure (information from ref. [3])

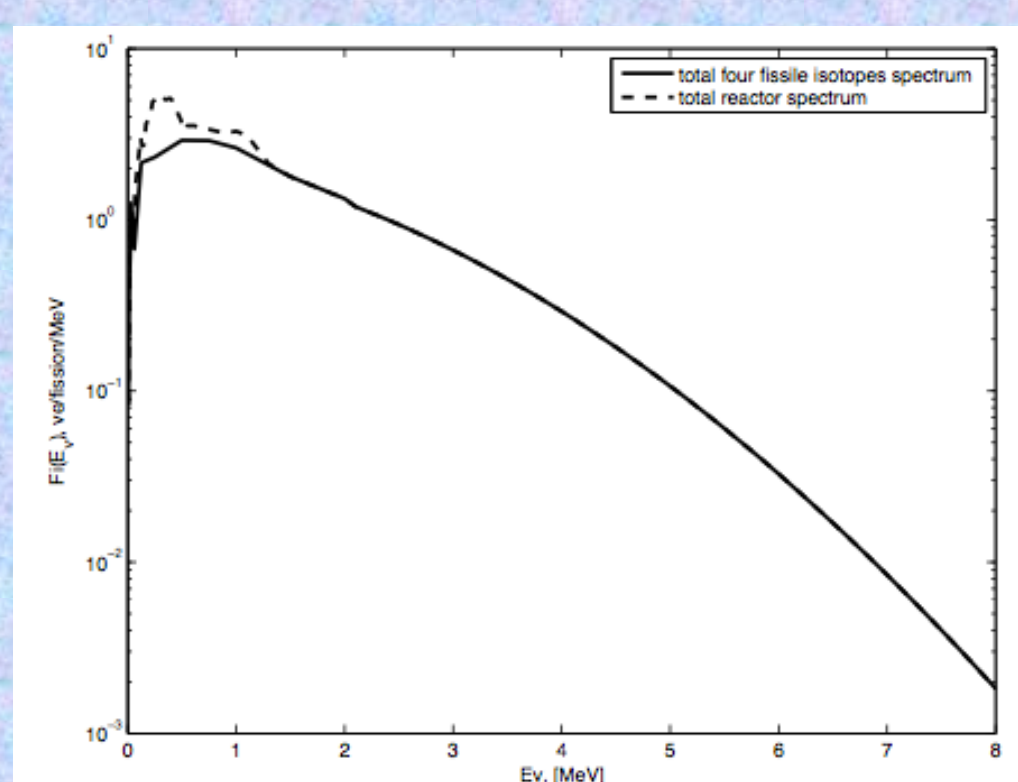


Fig. 3. total ν_e -yield per fission with and without neutron capture by ^{238}U .

Detector

CCD

The detector itself is composed by 6-10 scientific CCDs. These devices are fully depleted, back illuminated CCDs fabricated on high resistivity silicon specially designed for visible and near infrared detection. The low doping concentration together with a substrate voltage of 40 Volts allows a depletion thickness of 250 μm which is twenty times larger than regular CCDs. This extra depletion region increases the detecting mass to 1-1.5g per detector what makes possible to use them as neutrino and dark matter detectors.

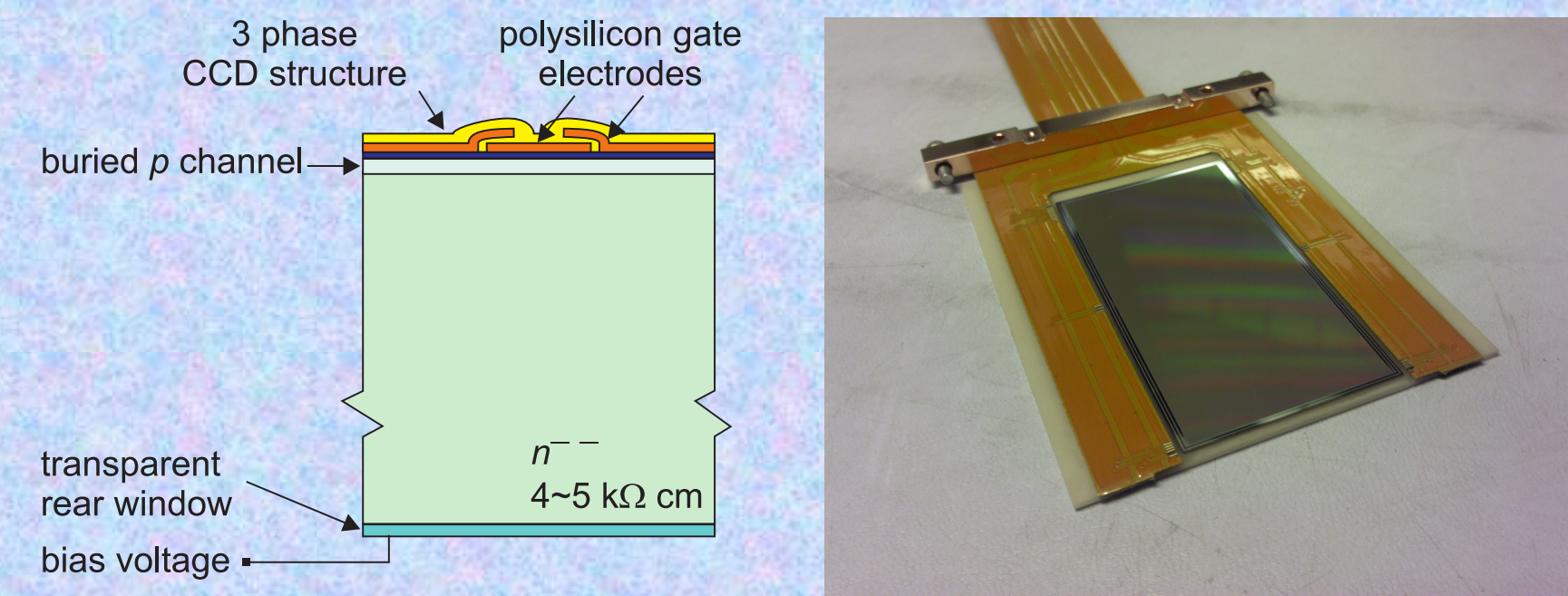


Fig. 4. Pixel cross section and CCD mounted on a low radiation background package.

CCD threshold energy

The threshold energy for this kind of scientific CCD is mainly given by the readout noise produced by its output amplifier. This noise can be reduced increasing the pixel time up to a limit of $2e=7eV$. The next figure shows the CCD readout noise as a function of the pixel time.

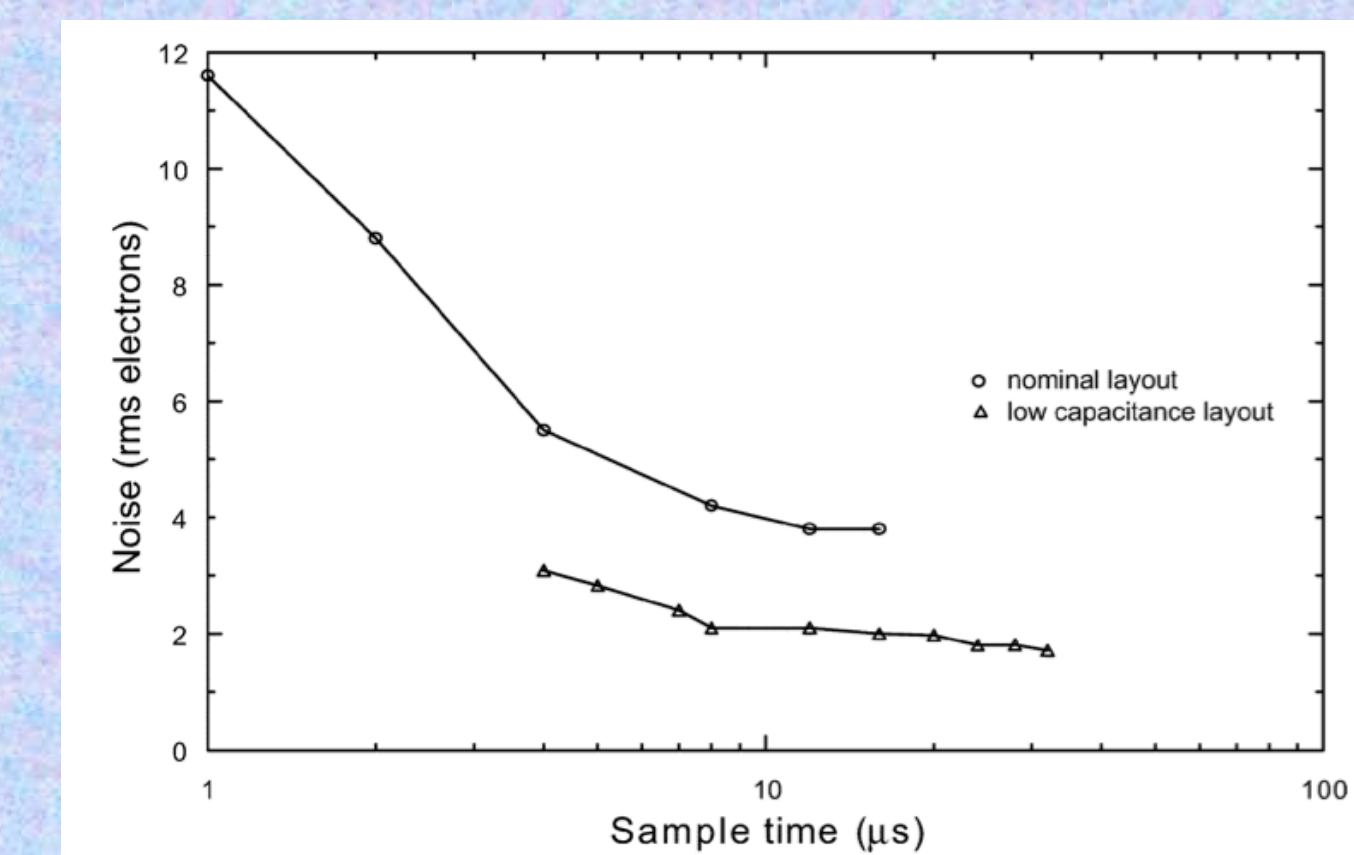


Fig. 5. CCD readout noise as a function of the pixel time

Mechanical Structure and peripheral Systems

The 6-10 CCDs are placed in a copper box that gives the thermal conductivity, mechanical support and provides the first layer of the background radioactivity shielding.

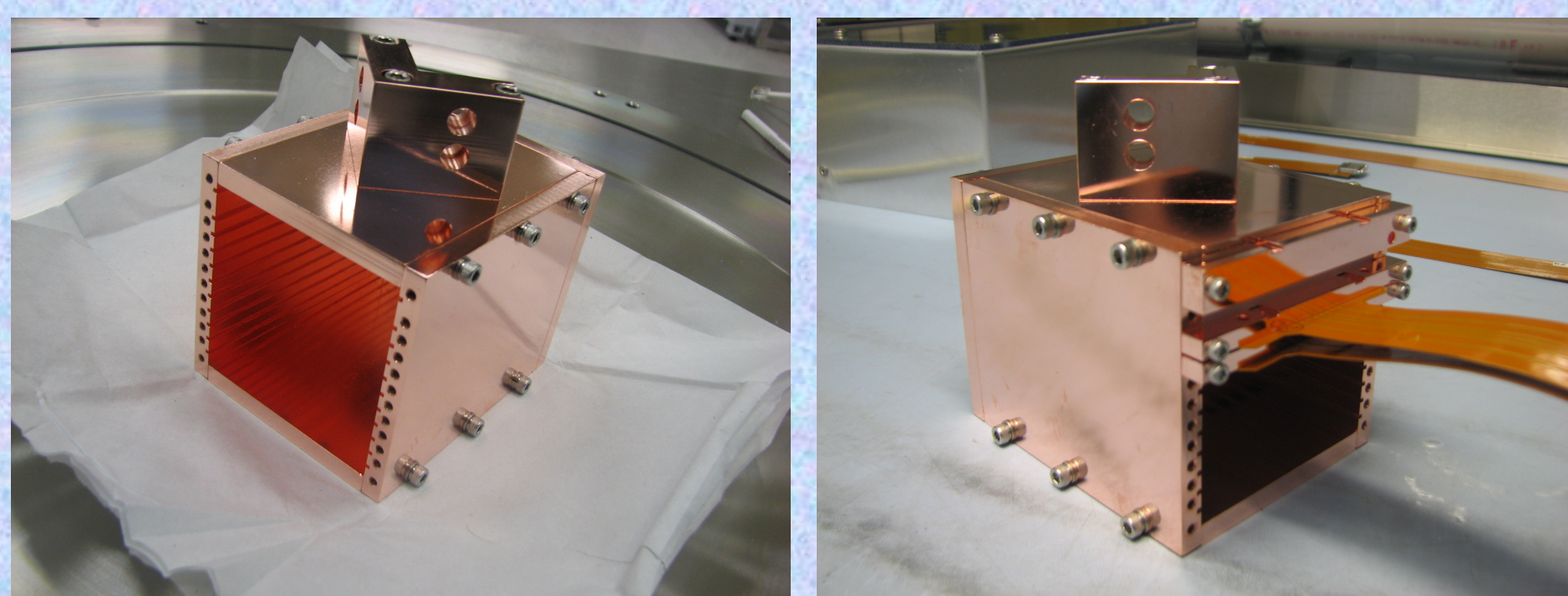


Fig. 6. Copper Box where the CCDs are placed.

The copper box goes inside a copper dewar with vacuum that prevents the condensation of water on the CCDs. The detectors are cooled to 143K for reducing the dark current generation. The cooling system is a cryostat using helium. The CCDs' signals go through the dewar wall by a VIB board that is connected to the readout system (Monsoon readout system).

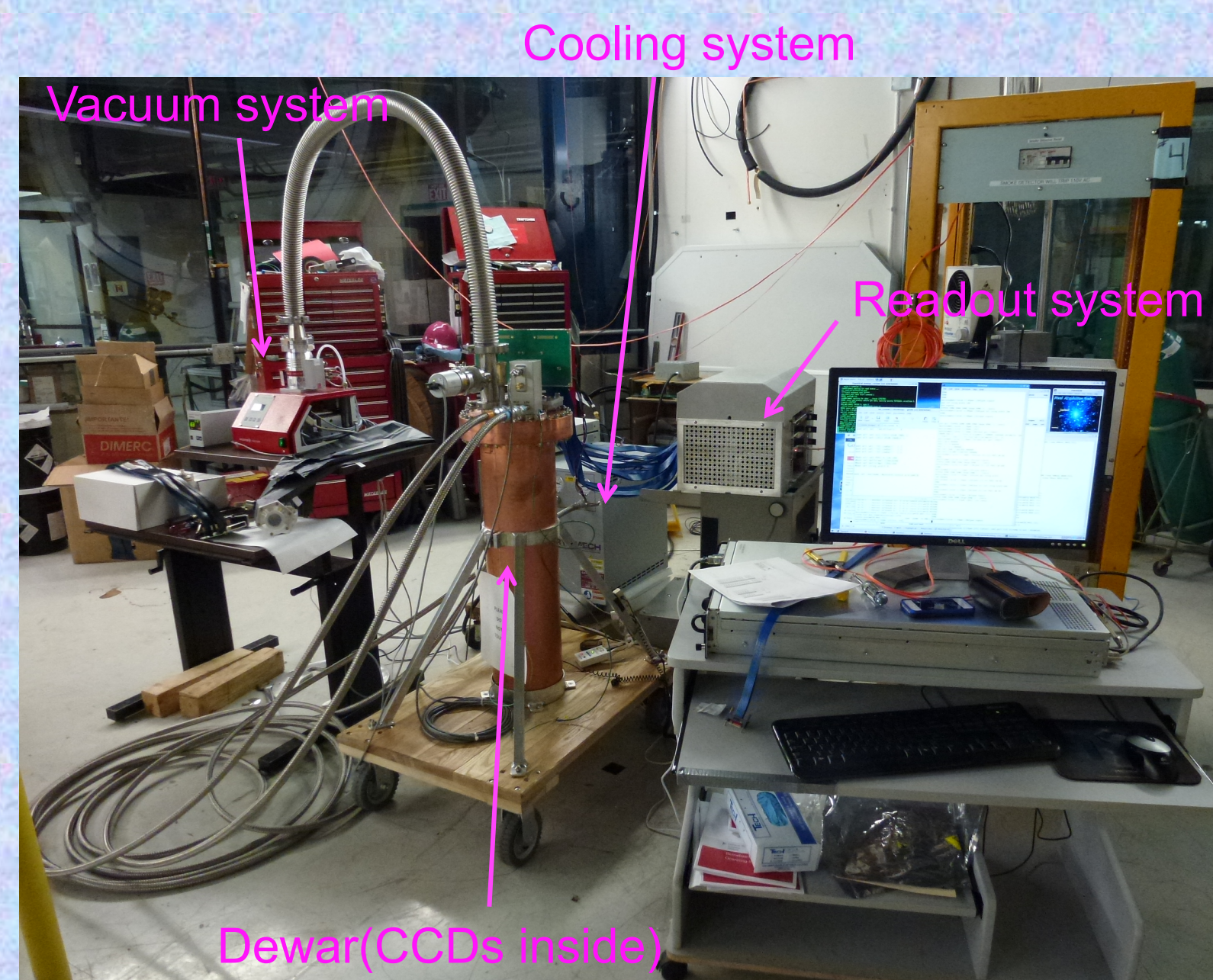


Fig. 7. CONNIE setup.

Shielding

The shielding is composed by three layers: outside borated polyethylene layer for cosmic neutrons moderation, then a 15 cm thick lead layer for photon rejection and an inner polyethylene layer for reduction of the neutron flux produced by muons in the lead.

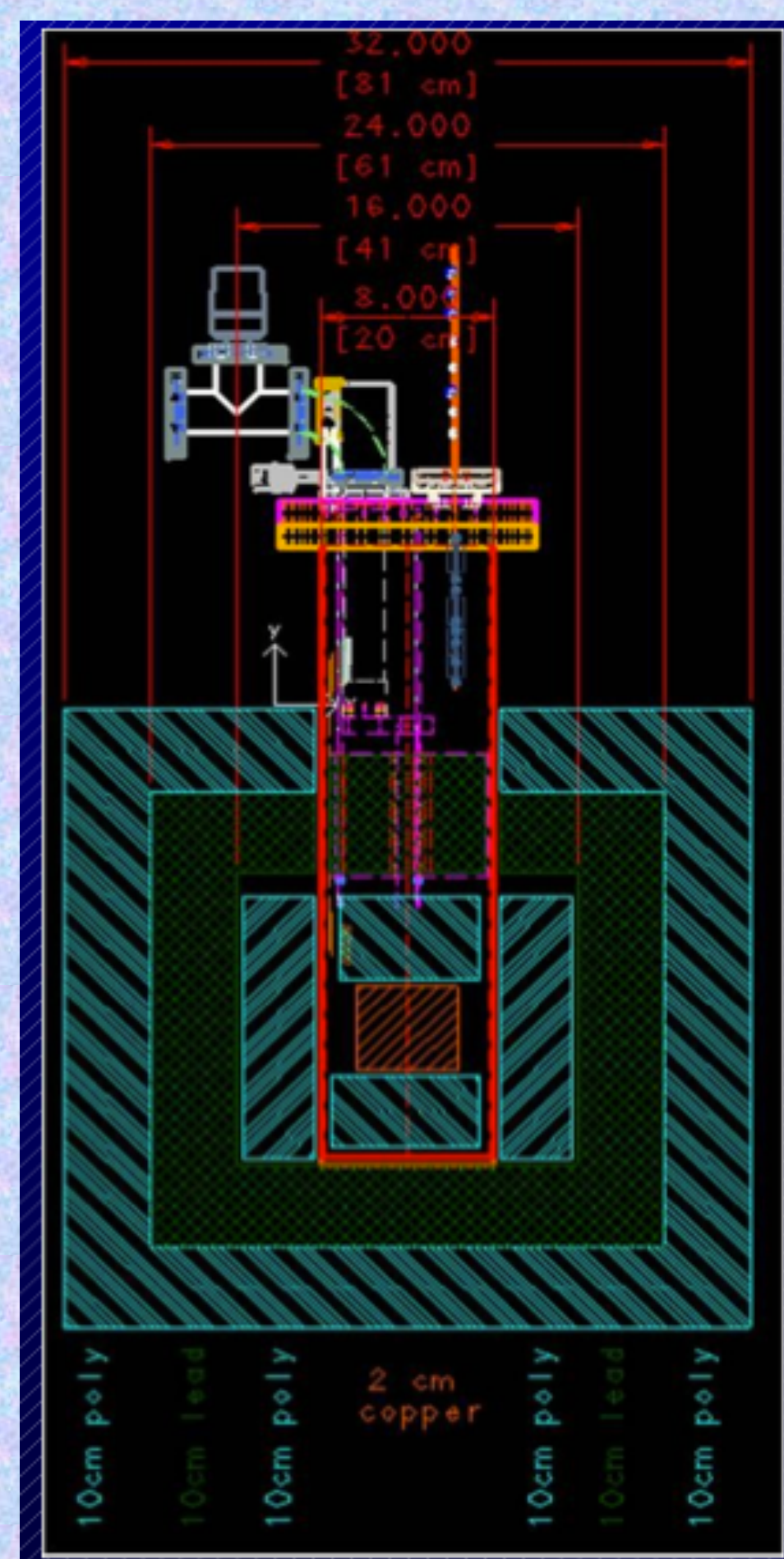


Fig. 8. Shielding.

Expected events rate in a 4GW reactor at L = 30m

Neutrino Flux

The detector will be installed in the Angra Nuclear Power Plant, in Angra dos Reis, Brazil. Approximately 3.12×10^{18} fissions per second are held in a reactor per 1MW of thermal power, so in a 4GW reactor 1.25×10^{20} are produced per second. As the reactor is an isotropic source of neutrinos, the neutrino flux at a distance L from the core is reduced by a factor of $4\pi L^2$, so the antineutrino flux at the detector is $1.25 \times 10^{20}/(4\pi L^2)$ times the total spectrum shown in fig. 3. The total flux of antineutrinos at the detector for all energies is 7.94×10^{12} $\nu^-/\text{cm}^2/\text{seg}$.



Fig. 9. Neutrino lab at Angra Nuclear Power Plant.

Event Spectrum

The expected event spectrum at the detector is computed for Silicon and Germanium, and compared to the results of Wong [1], for a reactor of 2.9 GW of thermal power at a distance of 28 m to the detector. In order to get the corresponding values for our setup at Angra Nuclear Plant, all the calculations must be multiplied by a factor of 1.2.

$$\frac{R}{dE_{rec}}(E_{rec}) = N_i \int_{\frac{E_{rec}}{2}}^{\infty} dE_\nu \Phi(E_\nu) \frac{d\sigma}{dE_{rec}}(E_\nu, E_{rec})$$

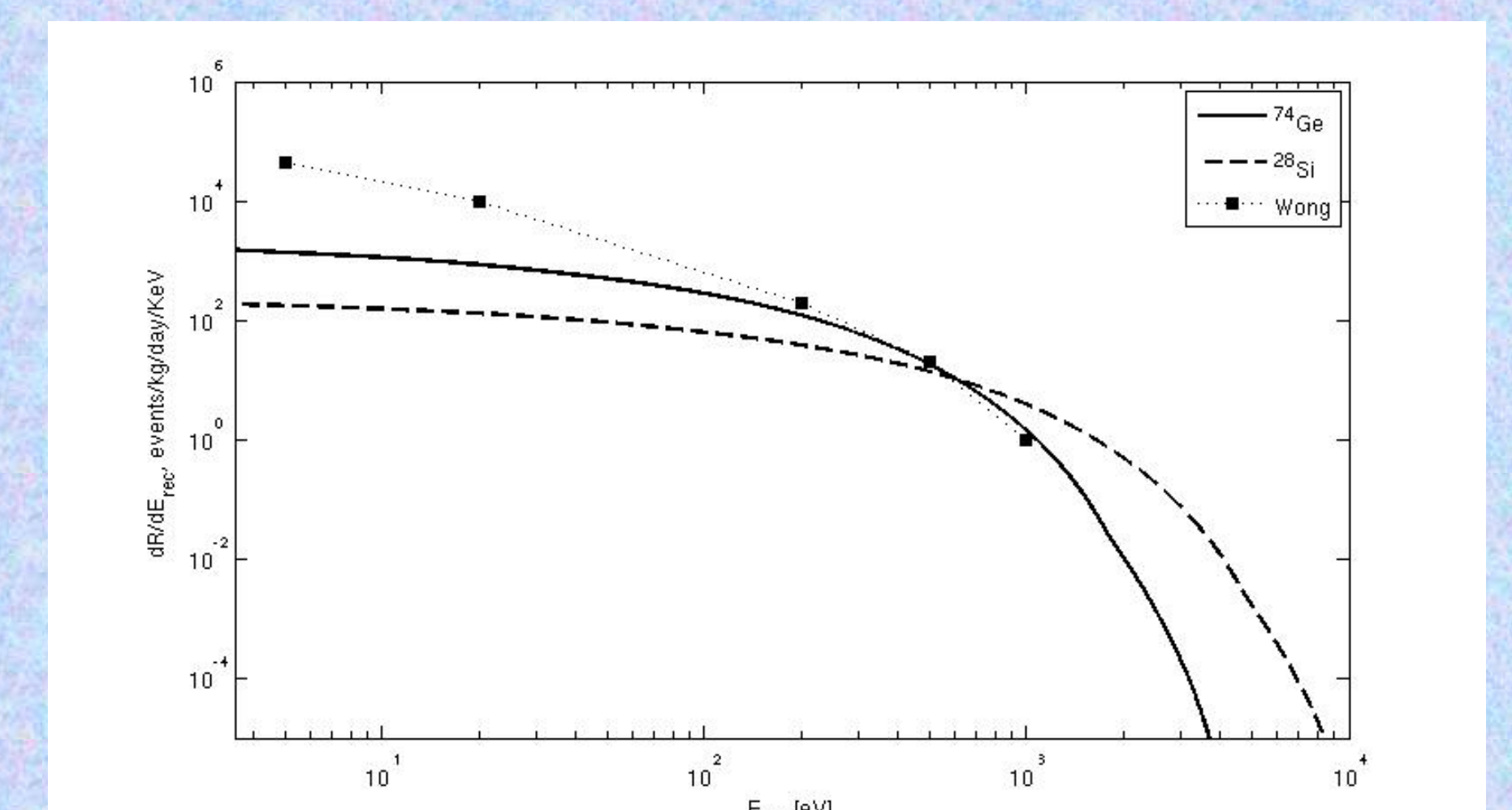


Fig. 10. Expected recoil spectrum for Si and Ge detectors.

The total number of events for 10g of silicon (6-10 CCDs) is around 0.33 events per day. The total expected event rate at all energies as a function of the detector's threshold energy is

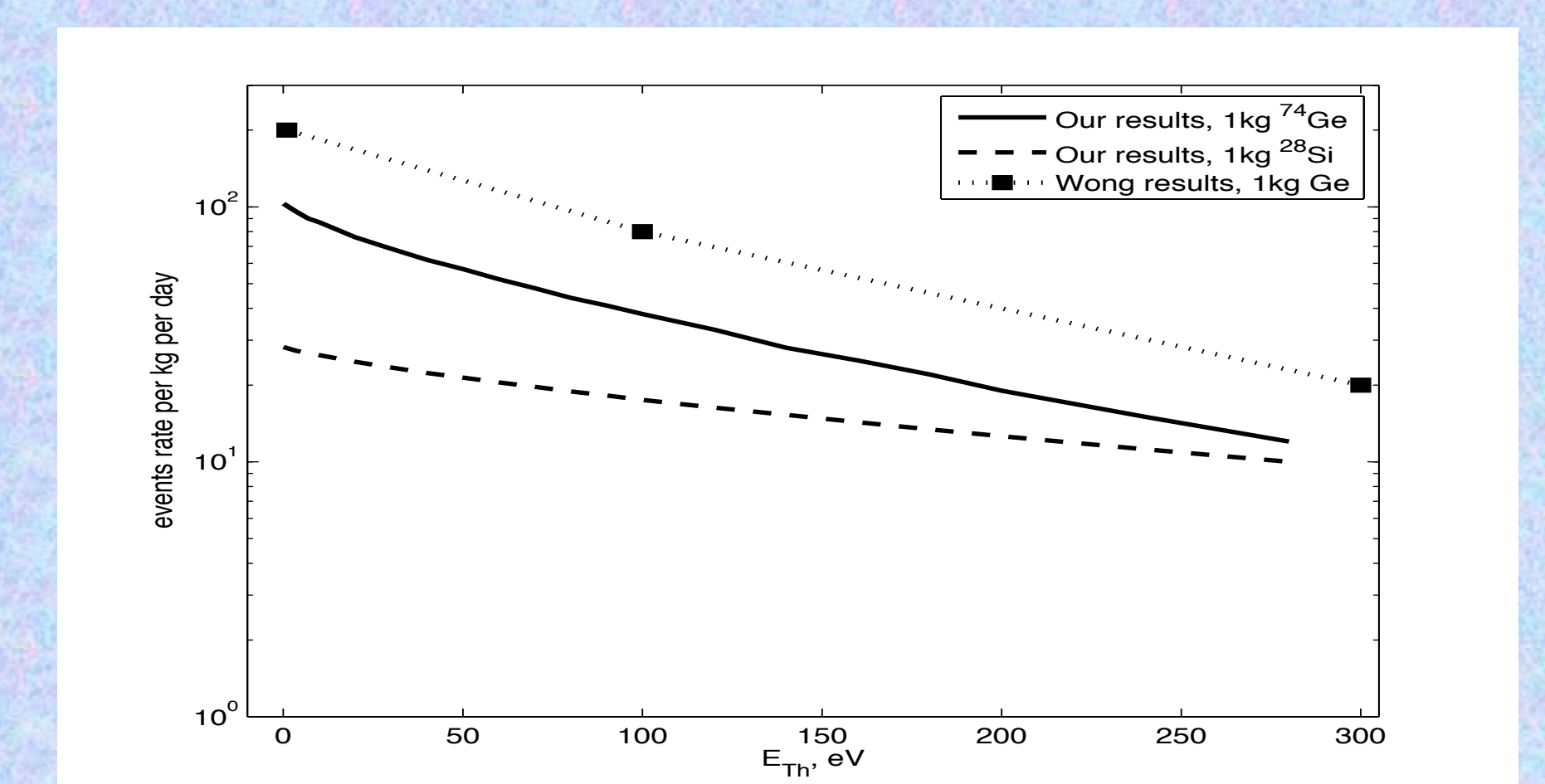


Fig. 11. Total number of events as a function of the energy threshold.

The next plot shows the minimum required neutrino energy as a function of the recoil energy:

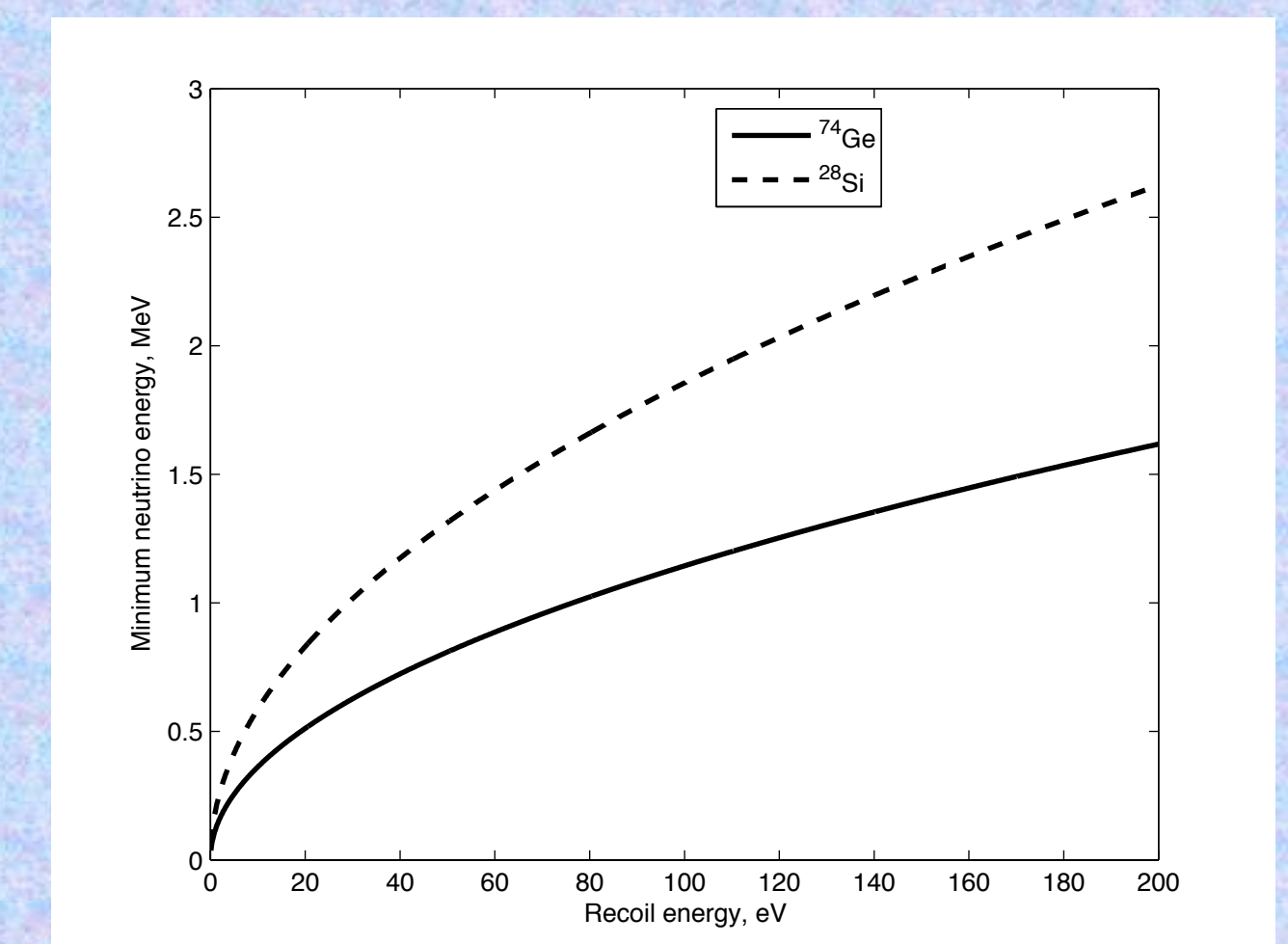


Fig. 12. Minimum required neutrino energy as a function of the recoil energy.

Conclusion

The potentiality of CCDs for detecting coherent neutrino-nucleus interactions is shown, and the main characteristics of the experiment and its setup are detailed.

References

- [1] Wong, H. T. et al., Research program towards observation of neutrino-nucleus coherent scattering, 2006.
- [2] Xin, B. et al., Production of Electron Neutrinos at Nuclear Power Reactors and the Prospects for Neutrino Physics, 2005. arXiv:hep-ex/0502001v3.
- [3] Wong, H. T. et al., Search of Neutrino Magnetic Moments with a High-Purity Germanium Detector at the Kuo-Sheng Nuclear Power Station, 2006.
- [4] Vogel, P.; Schenter, G. K., Reactor antineutrino spectra and their application to antineutrino-induced reactions. II, 1981.
- [5] Vogel, P.; Engel, J., Neutrino electromagnetic form factor, 1989.